Radio Interferometric Studies of Cool Evolved Stellar Outflows

A dissertation submitted to the University of Dublin
for the degree of Doctor of Philosophy

Eamon O'Gorman

Supervisor: Dr. Graham M. Harper

Trinity College Dublin, September 2013

School of Physics
University of Dublin
Trinity College

Declaration

I declare that this thesis has not been submitted as an exercise for a degree at this or any other university and it is entirely my own work.

I agree to deposit this thesis in the University's open access institutional repository or allow the library to do so on my behalf, subject to Irish Copyright Legislation and Trinity College Library conditions of use and acknowledgement.

Name: Your Name

Signature: ..... **Date:** .....

Summary

You should write a nice summary here...

A dedication if you wish...

Acknowledgements

Some sincere acknowledgements...

List of Publications

Refereed

1. Richards, A. M. S., Davis, R. J., Decin, L., Etoka, S., Harper, G. M., Lim, J. J., Garrington, S. T., Gray, M. D., McDonald, I., **O'Gorman, E.**, Wittkowski, M.
   "e-MERLIN resolves Betelgeuse at wavelength 5 cm"
   Monthly Notices of the Royal Astronomical Society Letters, 432, L61 (2013)

2. **O'Gorman, E.**, Harper, G. M., Brown, J. M., Brown, A., Redfield, S., Richter, M. J., and Requena-Torres, M. A.
   "CARMA CO(J = 2 - 1) Observations of the Circumstellar Envelope of Betelgeuse"
   The Astronomical Journal, 144, 36 (2012)

3. Sada, P. V., Deming, D., Jennings, D. E., Jackson, B. K., Hamilton, C. M., Fraine, J., Peterson, S. W., Haase, F., Bays, K., Lunsford, A., and **O'Gorman, E.**
   "Extrasolar Planet Transits Observed at Kitt Peak National Observatory"
   Publications of the Astronomical Society of the Pacific, 124, 212 (2012)

4. Sada, P. V., Deming, D., Jackson, B. K., Jennings, D. E., Peterson, S. W., Haase, F., Bays, K., **O'Gorman, E.**, and Lundsford, A.
   "Recent Transits of the Super-Earth Exoplanet GJ 1214b"
   The Astrophysical Journal Letters, 720, L215 (2010)

Non-Refereed

1. **O'Gorman, E.**, & Harper, G. M.
   "What is Heating Arcturus' Wind?",
   Proceedings of the 16th Cambridge Workshop on Cool Stars, Stellar Systems and the Sun. Astronomical Society of the Pacific Conference Series, 448, 691 (2011)

Contents

List of Figures

List of Tables

1 Introduction

Stellar winds in general ism planets

Empirical studies are vital to constrain physical parameters of the mass loss process.

1.1 Motivation for Researching Cool Evolved Stellar Outflows

Mass-loss from non-coronal spectral-type K through mid-M evolved stars plays a crucial role in galactic evolution and ultimately provides part of the material required for the next generation of stars and planets. This mass-loss occurs via a cool ($T_e \lesssim 10^4\,K$) wind with terminal velocities typically less than the photospheric escape velocity ($10 \leq v_\infty \leq 50\,\mathrm{km\,s^{-1}}$). The mass-loss rates for the red giants are significant, typically $10^{-9} - 10^{-11}\,M_\odot\,\mathrm{yr}^{-1}$, and are even higher for the more short-lived red supergiants, typically $10^{-4} - 10^{-6}\,M_\odot\,\mathrm{yr}^{-1}$. This implies that a substantial fraction of the star's initial mass can be dispersed to the interstellar medium (ISM) during these post main sequence evolutionary stages (e.g., Schröder & Sedlmayr, 2001). Mass-loss from these stars is therefore a crucial factor governing stellar evolution (Chiosi & Maeder, 1986) and also in explaining the frequency of supernovae in the galaxy (van Loon, 2010). Despite the importance of this phenomenon, and decades of study, the mechanisms that drive winds from evolved spectral-type K through mid-M stars remain unclear (clearly laid out by Holzer & MacGregor 1985 but still unsolved, e.g., Crowley *et al.* 2009). There is insufficient atomic, molecular, or dust opacity to drive a radiation-driven outflow (Jones, 2008; Zuckerman *et al.*, 1995) and acoustic/pulsation models cannot drive the observed mass-loss rates (Sutmann & Cuntz, 1995). Ultraviolet (UV) and optical observations reveal an absence of significant hot wind plasma, and the winds are thus too cool to be Parker-type thermally-driven flows (e.g., Ayres *et al.*, 1981; Haisch *et al.*, 1980; Linsky & Haisch, 1979).

Magnetic fields are most likely involved in the mass-loss process, although current magnetic models are also unable to explain spectral diagnostics. Exquisite high signal-to-noise ratio (S/N) *Hubble Space Telescope* (HST) UV spectra have revealed that the 1-D linear Alfvén wave-driven wind models of the 1980s (e.g., Harper 1988; Hartmann & MacGregor 1980) are untenable (Harper *et al.*, 2001). These models predict chromospheres as integral parts of a turbulent, extended, and heated wind acceleration zone, but the theoretical line profiles and electron densities do not agree with the HST spectra, (e.g., Judge & Carpenter, 1998). A

new generation of theoretical models with outflows driven within diverging magnetic flux tubes have now emerged (Falceta-Gonçalves *et al.*, 2006; Suzuki, 2007) but these too are not yet in agreement with observations (Crowley *et al.*, 2009). It has also been suggested that the winds may be driven by some form of magnetic pressure acting on very highly clumped wind material (Eaton, 2008) but Harper (2010) does not find compelling evidence for this hypothesis. Progress in this field continues to be driven by observations which can test existing models and theories, and provide new insights and constraints into the mass-loss problem.

Why at Radio Wavelengths?

Understanding the dynamics and thermodynamics of the atmospheres of late-type evolved stars will ultimately lead to a broader understanding of their mass-loss processes. Red supergiants have extended atmospheres which contain a mixture of atoms, ions, molecules, and dust, and are an ideal test bed for ideas and theories of mass-loss. These atmospheres are so extended that the closest red supergiants can be spatially resolved and imaged at centimeter and millimeter-wavelengths, both in continuum emission and in molecular line emission. Such observations can yield direct measurements of the gas temperature, velocity, and atmospheric structure, which can be used to provide essential constraints on the mass-loss process. The red giants [excluding the asymptotic-giant-branch (AGB) red giants] on the other hand have less extended atmospheres which are dust free and contain only small abundances of molecules. They currently[1] cannot be spatially resolved at radio wavelengths, but their partially ionized outflows can still be detected at these wavelengths, providing an area-averaged sweep through the atmospheres of these stars. The lack of spatial resolution prevents the direct measurement of the fundamental atmospheric properties. However, point source radio observations can still be compared against existing atmospheric models based on shorter wavelength observations (e.g., models based on optical and UV observations). Such radio observations sample further out in the star's atmosphere than optical and UV observations and can test the validity of and improve upon existing model atmospheres.

[1] ALMA will eventually be capable of spatially resolving the atmospheres of red giants.

1.2 The Nature of Cool Evolved Stellar Outflows

The study of stellar outflows from cool evolved stars began with the discovery of blue-shifted absorption features in strong resonance lines from a number of bright red supergiants (Adams & MacCormack, 1935). They attributed these features to gradually expanding envelopes, even though the expansion speed velocity was small ($\sim 5\,\mathrm{km\,s^{-1}}$) and much less than the photospheric escape velocity. Spitzer (1939) analyzed similar data and devised a *fountain model* for the atmospheres of red supergiants. In this model, radiation drives matter upwards from the photosphere until at some height, the ionization state of the matter changes, causing the radiation force to drop so that the matter falls back onto the star. Definitive evidence for mass loss from cool evolved stars came from Deutsch (1956) who observed a system which contained an M5 giant (i.e., α Her) and a G5 dwarf. They found that the same blue-shifted absorption feature was present in the spectrum of both stars at orbital phases which indicated that both stars were enveloped in material which had been emitted from the M5 giant. The inferred expansion velocity at the distance of the G5 dwarf was sufficient to escape the system, thus confirming that matter was escaping the gravitational potential of the α Her system.

uv spectra shows gradual acceleration Bow shocks (image decin)

An important discovery in late-type evolved stellar atmospheres resulted from the first ultraviolet survey of such stars using the *International Ultraviolet Explorer* (IUE). The survey revealed a 'transition region dividing line' in the giant branch near spectral type K1 III which separates these stars based on the properties of their atmospheres (Linsky & Haisch, 1979). Stars blueward of the dividing line were found to possess chromospheres and transition regions like the Sun, while stars on the red side were found to possess chromospheres and cool winds. X-ray observations showed that this dividing line extended to coronal emission (Ayres *et al.*, 1981). Around the same time, another class of late-type evolved star emerged which showed signs of possessing both a transition region and a cool wind (e.g., Reimers, 1982). Many of these so-called 'hybrid atmosphere' stars now

also show evidence for coronal emission, albeit much weaker than on the blue side of the dividing line (Ayres *et al.*, 1997; Dupree *et al.*, 2005).

One important property of cool evolved star winds gleaned from UV spectra is that, for the most part, the red giant winds accelerate in a quasi-steady manner and are not the result of ballistic ejecta as shown by the increase of wind scattering absorption velocity with optical depth in Fe II lines (Carpenter *et al.*, 1999).

1.3 Basic Concepts of Stellar Winds

bernoulli (casinelli p95) parker lamers review paper

1.4 Stellar Winds Across the HR Diagram

mass loss picture across the HR diagram Maybe give image in transfer of winds across HR diagram cranmer pictures mathews solar unexplained description suzuki intro for the sun

1.5 Red Giant and Red Supergiant Evolution

Stellar structure Internal and Atmospheric table of scale heights, pressure/density scale height for the Sun, Arctutus, Aldaberan, Betelgeuse Betelgeuse very large scale height resulting in the presence of no more than a few giant and stable convection cells at photospheric level (Schwarzschild 1975, Chiavassa et al. 2010) i.e. schwarychild criteria MOLsphere: explain what it is [tsuji (1988)] Circumstellar environments (Lamers and Cassinelli CO) 'The past present and future evolution of red supergiants' workshop 2012, meynet Stellar Evolution -HR diagram (Boyajian 2013 (Bee's Knees! See print out pile 3)) suzuki paper- why rgs have no corona reimers mass loss forulae gravity modes h and he burning (nature) Ayres paper (buried chromosphere)

1.6 Radio Emission from Stellar Atmospheres

give fundamental frequencies

radio hr diagram gudel

$$F_\nu \approx 0.1 \left(\frac{T_b}{10^6\,K}\right) \left(\frac{\nu}{1\,\mathrm{GHz}}\right)^2 \left(\frac{r}{10^{11}\,\mathrm{cm}}\right)^2 \left(\frac{1\,\mathrm{pc}}{d}\right)^2 \quad \mathrm{mJy} \qquad (1.1)$$

(Güdel, 2002)

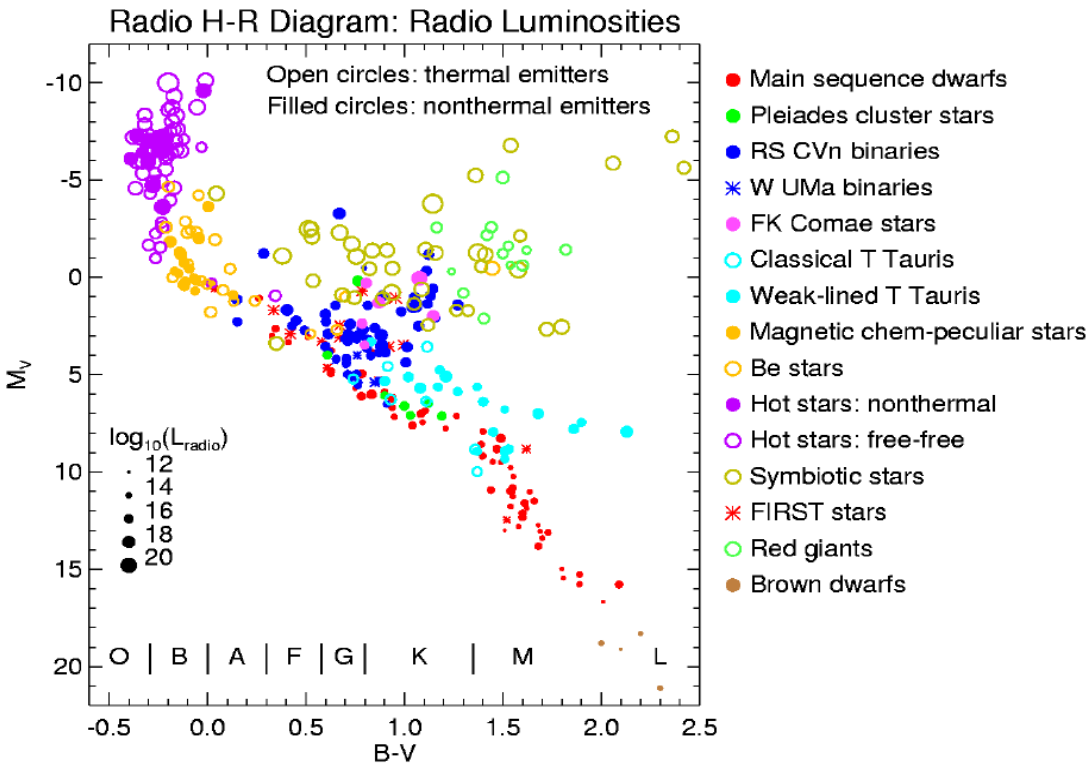

Figure 1.1

1.6.1 Free-free Emission

1.6.2 Molecular Line Emission

1.6.3 Other Emission Mechanisms

Recombination Line Emission

Non-Thermal Emission

1.7 Radio Observations of Stellar Atmospheres

In the following sections we present the basic definitions used to describe radio observations of stellar atmospheres. We define the *brightness temperature* which is commonly used in radio astronomy to measure the brightness of a source, along with its relationship to the fundamental quantity measured by a radio telescope, the *flux density*. Focusing on thermal emission, we describe how the flux density varies with frequency when observing both optically thin and optically thick stellar atmospheres.

1.7.1 Brightness Temperature

In thermodynamic equilibrium the spectral distribution or brightness, B_ν, of the radiation of a black body with temperature T_e is given by the Planck law

$$B_\nu(T_e) = \frac{2h\nu^3}{c^2}\frac{1}{e^{h\nu/kT_e} - 1} \tag{1.2}$$

and has units of flux per frequency interval per solid angle. One can easily switch to a wavelength scale using $B_\nu d\nu = B_\lambda d\lambda$. When $h\nu \ll kT_e$ Equation 1.2 becomes the *Rayleigh-Jeans Law*

$$B_\nu(T_e) = I_\nu(T_e) = \frac{2\nu^2 kT_e}{c^2}. \tag{1.3}$$

This equation does not contain Plank's constant and therefore is the classical limit of the Planck Law. We have also included the specific intensity, I_ν, here as it has the same units as the spectral brightness and for blackbody radiation, $I_\nu(T_e) = B_\nu(T_e)$. This equation is valid for all thermal radio sources except in the millimeter or sub-millimeter regime at low temperatures (Rohlfs & Wilson, 1996). In the Rayleigh-Jeans relation, the brightness is strictly proportional to the thermodynamic temperature of the black body. In radio astronomy it is customary to measure the brightness of an object by its *brightness temperature*, T_b. Therefore, the brightness temperature is the temperature at which a blackbody would have to be in order to reproduce the observed brightness of an object at

frequency ν and is defined as

$$T_{\rm b} = \frac{c^2}{2k\nu^2} I_\nu. \tag{1.4}$$

If $h\nu/kT \ll 1$ and if I_ν is emitted by a blackbody, then $T_{\rm b}$ is the thermodynamic temperature of the source. If other processes are responsible for the emission or if the frequency is so high that Equation 1.3 is not valid, then $T_{\rm b}$ is different from the thermodynamic temperature of a black body.

The equation of radiative transfer describes the change in specific intensity of a ray along the line of sight in a slab of material of thickness ds

$$\frac{dI_\nu}{ds} = \varepsilon_\nu - \kappa_\nu I_\nu, \tag{1.5}$$

where ε_ν and κ_ν are the emissivity (in $\mathrm{erg\,s^{-1}\,cm^{-3}\,Hz^{-1}\,sr^{-1}}$) and the absorption/opacity coefficient (in $\mathrm{cm^{-1}}$) of the plasma. In thermodynamic equilibrium the radiation is in complete equilibrium with its surroundings and the brightness distribution is described by the Planck function

$$\frac{dI_\nu}{ds} = 0, \qquad I_\nu = \frac{\varepsilon_\nu}{\kappa_\nu} = B_\nu(T_e). \tag{1.6}$$

Equation 1.5 can be solved by first defining the optical depth, $d\tau_\nu$, as

$$d\tau_\nu = -\kappa_\nu ds, \tag{1.7}$$

and then integrated by parts between 0 to s, and τ to 0, to give

$$I(s) = I(0)e^{-\tau(s)} + \int_{\tau(s)}^{0} e^{-\tau} \frac{\varepsilon_\nu}{\kappa_\nu} d\tau. \tag{1.8}$$

The second term within the integral is known as the source function, S_ν, and this can be taken outside of the integral in the case of a homogeneous source, i.e., one for which both the emissivity and absorption coefficient are constant along the ray path. The solution then to the equation of radiative transfer for a homogeneous source is

$$I_\nu = I_0 e^{-\tau} + \frac{\varepsilon_\nu}{\kappa_\nu}(1 - e^{-\tau}). \tag{1.9}$$

Using Equations 1.4 and 1.6 one obtains

$$T_b = T_0 e^{-\tau} + T_e(1 - e^{-\tau}). \tag{1.10}$$

This equation assumes thermodynamic equilibrium and so only holds for a thermal source. If T_e is replaced with $T_{\rm eff} = h\nu/k$ then this equation becomes valid for a homogeneous nonthermal source, i.e.,

$$T_b = T_0 e^{-\tau} + T_{\rm eff}(1 - e^{-\tau}). \tag{1.11}$$

For an isolated thermal source, there are two limiting cases:

$$T_b = T_e \quad \text{(i.e., for optically thick } \tau \gg 1) \tag{1.12}$$

and

$$T_b = \tau T_e \quad \text{(i.e., for optically thin } \tau \ll 1). \tag{1.13}$$

In these equations, T_e can also be replaced by $T_{\rm eff}$ if the radio emission emission is non-thermal. Also, these equations are only valid if the source is spatially resolved. If the source is unresolved then an upper limit to $T_e/T_{\rm eff}$ is found.

1.7.2 Brightness Temperature and Flux Density

The flux density, F_ν, is a fundamental quantity measured by a radio telescope and is usually measured in Janskys (Jy) where $1\,\mathrm{Jy} = 1 \times 10^{-26}\,\mathrm{W\,m^{-2}\,Hz^{-1}}$. The observed flux density measured by the radio telescope is

$$F_\nu = \int_\Omega I_\nu \, d\Omega \tag{1.14}$$

where Ω is the solid angle subtended by the star. The radio emission from evolved cool stars is almost purely thermal and so Equation 1.14 becomes

$$F_\nu = \frac{\pi R_\star^2}{d^2} \frac{2k\nu^2 T_b}{c^2}. \tag{1.15}$$

The angular diameter of a star in radians is $\phi_\star = 2R_\star/d$ and so

$$F_\nu = \frac{\pi k \phi_\star^2 T_b}{2\lambda^2} \tag{1.16}$$

If $\phi_\star$ has major and minor axes $\phi_{\rm maj}$ and $\phi_{\rm min}$ then

$$T_b(K) = 1.96 F_\nu(\mathrm{mJy}) \left(\frac{\lambda}{\mathrm{cm}}\right)^2 \left(\frac{\phi_{\rm min}}{\mathrm{arcsec}} \frac{\phi_{\rm min}}{\mathrm{arcsec}}\right)^{-1}. \tag{1.17}$$

Therefore, if an optically thick stellar atmosphere can be spatially resolved (i.e., $\phi_{\rm maj}$ and $\phi_{\rm min}$ can be measured) then the flux density at a particular wavelength tells gives the brightness temperature and therefore the electron temperature. Unfortunately, the number of stars that can have their atmospheres spatially resolved at radio wavelengths is low due to their relatively small angular diameters. However, different layers of stellar atmospheres can still be probed due to the nature of the free-free radio opacity which is discussed in the next section.

1.7.3 Thermal Free-free Radio Opacity

In Section 1.6.1 we derived an expression for the thermal free-free emissivity of an ionized gas. Since we assumed LTE at some temperature T, we can use Kirchoff's law to find the thermal radio free-free opacity (absorption coefficient):

$$\kappa_\nu^{ff} = \frac{\epsilon_\nu^{ff} c^2}{2kT_e\nu^2} \tag{1.18}$$

Substituting in Equation **??** then gives a value for the radio opacity which is corrected for stimulated emission

$$\kappa_\nu^{ff} = \frac{0.018 Z^2 n_e n_i g_{ff}(\nu, T_e)}{T_e^{1.5}\nu^2} \tag{1.19}$$

The Gaunt factor is slightly dependent on temperature and frequency and at cm-wavelengths is given by

$$g_{ff}^{cm} = 11.96 T_e^{0.15} \nu^{-0.1} \tag{1.20}$$

(Altenhoff *et al.*, 1960), while in the sub-millimeter regime it is slightly different

$$g_{ff}^{sub-mm} = 24.10 T_e^{0.26} \nu^{-0.17} \tag{1.21}$$

(Hummer, 1988). The abundant species in the atmospheres of cool evolved stars are either neutral or single ionized so that $Z = 1$ and $n_e = n_i$. Focusing on

centimeter wavelengths, the radio opacity is then

$$\kappa_\nu^{ff} = \frac{0.212 n_e^2}{T_e^{1.35}\nu^{2.1}} \qquad \mathrm{cm}^{-1}. \tag{1.22}$$

Therefore, the free-free opacity increases towards lower frequencies as $\kappa_\nu^{ff} \propto \nu^{-2.1}$ (or longer wavelengths as $\kappa_\lambda^{ff} \propto \lambda^{2.1}$). This means that the optical depth, $\tau_\lambda = \int \kappa_\lambda dr$, also increases towards longer wavelengths implying that the effective radius (i.e., the radius where $\tau_\lambda = \tau_{\mathrm{radial}}$) will increase with longer wavelengths. As a result, different layers of unresolved stellar atmospheres can be probed by observing them at different radio wavelengths.

In LTE, the solution to the equation of radiative transfer (i.e, Equation 1.9) for a plasma with no background source can be written as

$$I_\nu = B_\nu(1 - e^{-\tau}). \tag{1.23}$$

An example of such a source is an isolated H II region. At long enough wavelengths the H II region becomes opaque so that $\tau_\nu \gg 1$. Equation 1.23 then tells us that the spectrum approaches that of a black body with a flux density varying as $F_\nu \propto \nu^2$. At short wavelengths where $\tau_\nu \ll 1$, the H II region is almost transparent, and the flux density becomes

$$F_\nu \propto \frac{2kT_e\nu^2}{c^2}\tau_\nu \propto \nu^{-0.1}. \tag{1.24}$$

These two scenarios are shown in Figure ?? along with the point where these two slopes intersect which corresponds to the frequency at which $\tau \simeq 1$. When the radio spectrum is plotted on a log-log plot as in Figure 1.2, the spectral slope is referred to as the spectral index, α, and is defined:

$$\alpha = \frac{d\log F_\nu}{d\log \nu}. \tag{1.25}$$

1.7.4 Radio Excess from Stellar Outflows

Cool evolved stars have ionized or partially ionized outflows which emit an excess of continuum emission at long wavelengths. This flux excess is due to thermal

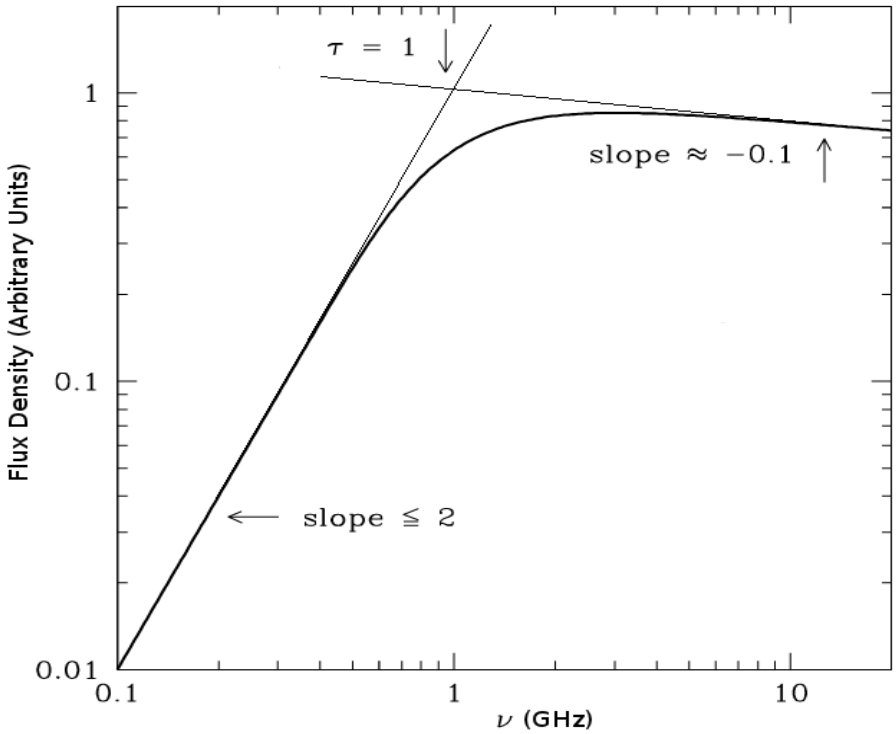

Figure 1.2: The radio spectrum for a hypothetical H II region with no background illuminating source. At long wavelengths the source becomes opaque and has a black body like spectrum with $\alpha = 2$. At short wavelengths where $\tau_\nu \ll 1$, the H II region is almost transparent and $\alpha = -0.1$. Image adapted from NRAO's *Essential Radio Astronomy* course.

free-free emission and is measured relative to the expected photospheric radio flux. If the atmosphere only consisted of a static homogeneous isothermal chromosphere then the radio spectrum would be the summation of the Rayleigh-Jeans tail of the Planck function from the photosphere and the H II spectrum discussed in the previous section. At long wavelengths then, this spectrum would again have a power law of slope $F_\nu \propto \nu^2$. Cool evolved stellar atmospheres cannot in general be described by this simple model because they possess stellar winds which are escaping the gravitational potential of the star. The atmospheric density thus varies with distance from the star. In this section we briefly outline a simple analytical model for the centimeter radio flux for a star with a isothermal, constant velocity and ionization fraction wind. In Chapter **??** we relax some of

these assumptions about the atmosphere's properties to derive a more complete description of the centimeter radio spectrum for these stars.

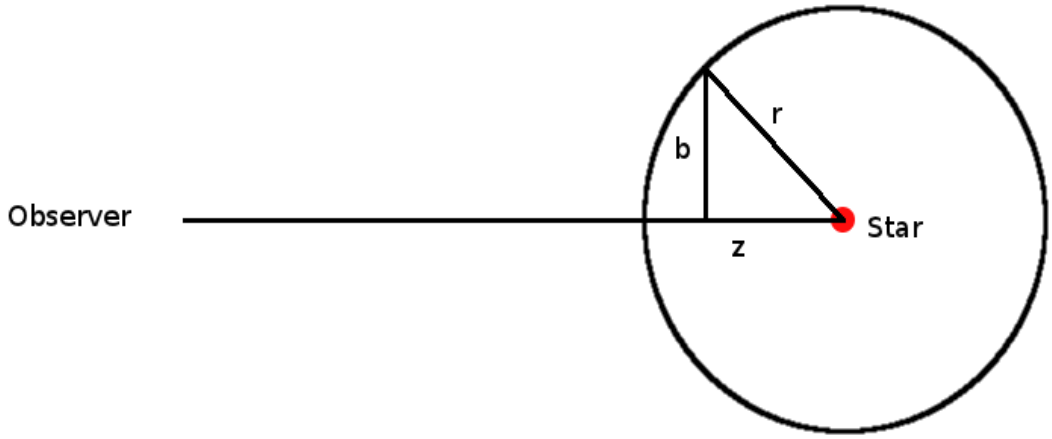

Figure 1.3: In spherical geometry the observer integrates along a ray path in the z direction, with impact parameter b, to calculate the total optical depth τ_ν, at a frequency ν.

To calculate the optical depth, we assume spherical geometry and integrate along a ray in the z direction with impact parameter b, as shown in Figure ??. The total optical depth at a frequency ν is then

$$\tau_\nu = \int_{-\infty}^{\infty} \kappa_\nu dz \tag{1.26}$$

where the opacity is defined in Equation 1.22. For a constant velocity the electron density is just $n_e(r) = n_e(r_0)^2(r_0/r)^2$ and so the optical depth can be written as

$$\tau_\nu = \frac{0.212 n_e(r_0)^2 r_0^4}{T^{1.35}\nu^{2.1}} \int_{\infty}^{\infty} \frac{dz}{(b^2+z^2)^2} \tag{1.27}$$

The solution to this integral is given by

$$\int_{-\infty}^{\infty} \frac{dz}{(b^2+z^2)^{A/2}} = b^{1-A}\sqrt{\pi}\frac{\Gamma(A/2-1/2)}{\Gamma(A/2)} \tag{1.28}$$

and so the total optical depth along a ray with impact parameter b is:

$$\tau_\nu = \frac{C}{b^3} \qquad \text{where} \quad C = \frac{0.333 n_e(r_0)^2 r_0^4}{T^{1.35}\nu^{2.1}} \tag{1.29}$$

To calculate the flux density we use Equation 1.14 and assume that the source function is given by the Planck function in the Rayleigh-Jeans approximation:

$$F_\nu = \frac{2\pi}{d^2}\frac{2\nu^2 kT}{c^2}\int_0^\infty (1 - e^{-C/b^3})bdb \tag{1.30}$$

This integral can be solved using the following expression

$$\int_0^\infty y^{v-1}(1 - e^{-uy^p})dy = \frac{-1}{|p|}u^{-v/p}\Gamma\left(\frac{v}{p}\right), \tag{1.31}$$

which is given in Gradshteyn & Ryzhik (1994). The solution to our integral is then $1.339C^{2/3}$ and so the total flux density can be written as

$$F_\nu = \frac{1.24 \times 10^{-16} n_e(r_0)^{4/3} r_0^{8/3} T^{0.1} \nu^{0.6}}{d^2} \qquad \text{Jy}. \tag{1.32}$$

This equation shows that the expected spectral index for an isothermal constant velocity and ionization fraction stellar outflow (i.e., a constant property wind) is $\alpha = 0.6$.

The free-free emission from evolved cool stars is weak (usually less than 1 mJy at $\lambda > 3$ cm) and therefore only a handful of these stars have known radio spectral indices at long wavelengths. The small number of such stars whose spectral indices are known have values which are greater than 0.6 (e.g. Drake & Linsky, 1986) due the assumptions in the constant property wind model being too simplistic. Betelgeuse is by far the best studied evolved cool star at radio wavelengths and its radio spectrum is shown in Figure 1.4 (Newell & Hjellming, 1982). Its spectral index clearly deviates from 0.6. In Chapter **??** we derive a new version of Equation 1.32 which accounts for a thermal gradient in the outflow along with flow acceleration. Nevertheless, Figure 1.4 is a good example of the radio flux excess which is present for all all cool evolved. Even though the observed flux density decreases to longer wavelengths, the excess increases relative to the expected photospheric flux as clearly seen in Figure 1.4.

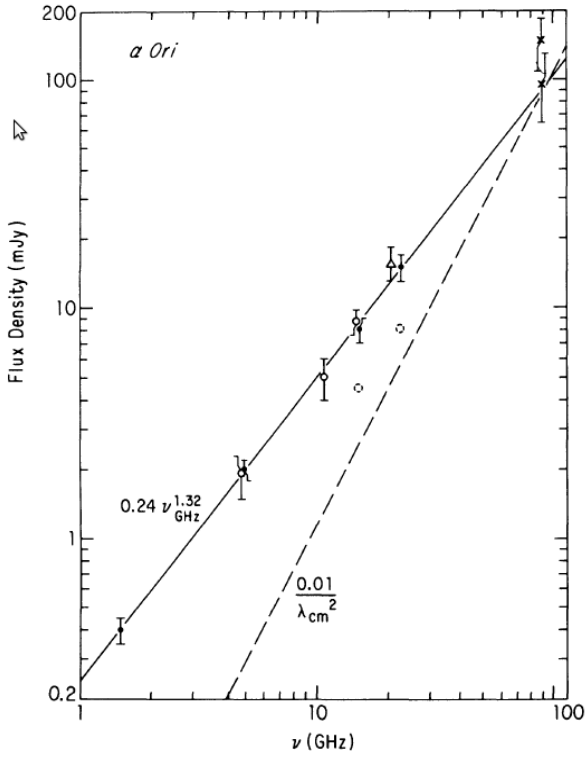

Figure 1.4: Example of a cool evolved star's radio flux excess, which is a direct result of their ionized atmospheres. Here, multi-wavelength radio observation of Betelgeuse are plotted along with a best fit power law indicating a spectral index of $\alpha = 1.32$ (Newell & Hjellming, 1982). Even though the observed flux density decreases at longer wavelengths, the excess increases relative to the expected photospheric flux (dashed line).

1.8 Goals of this Thesis

A

List of Abbreviations Used in this Thesis.

Table A.1: List of Abbreviations

First entry	Second entry
BIMA	Berkeley Illinois Maryland Association
CARMA	Combined Array for Research in Millimeter-wave Astronomy
CSE	Circumstellar Envelope
DDT	Director's Discretionary Time
e-MERLIN	e-Multi-Element Radio Linked Interferometer Network
FOV	Field of View
GREAT	German Receiver for Astronomy at Terahertz Frequencies
HPBW	Half Power Beamwidth
HST	Hubble Space Telescope
IOTA	Infrared Optical Telescope Array
IR	Infrared
IRAM	Institut de Radioastronomie Millimétrique
IUE	International Ultraviolet Explorer
LSR	Local Standard of Rest
MEM	Maximum Entropy Method
OVRO	Owens Valley Radio Observatory
RFI	Radio Frequency Interference
S/N	signal-to-noise ratio

Continued on next page

Table A.1 – *Continued from previous page*

First entry	**Second entry**
SOFIA	Stratospheric Observatory for Infrared Astronomy
SMA	Submillimeter Array
UV	Ultraviolet
VLA	Karl G. Jansky Very Large Array
VLBA	Very Long Baseline Array
VLT	Very Large Telescope

B

Ambipolar Diffusion Heating

Considering a steady flow accelerating in an inertial frame, the equation of motion can be written as

$$\rho_n \boldsymbol{a}_n = \rho_n \boldsymbol{g} + \boldsymbol{f}_d \tag{B.1}$$

for the neutral species n, and

$$\rho_i \boldsymbol{a}_i = \rho_i \boldsymbol{g} - \boldsymbol{f}_d + \boldsymbol{f}_L \tag{B.2}$$

for the ion species, i. The flow acceleration is defined as $\boldsymbol{a} \equiv (\boldsymbol{v}.\nabla)\boldsymbol{v}$ and the gravitational acceleration is $\boldsymbol{g} \equiv \nabla(GM_\star/r)$. The volumetric drag force of the ions on the neutrals is defined as

$$\boldsymbol{f}_d = \gamma \rho_n \rho_i (\boldsymbol{v}_i - \boldsymbol{v}_n) \tag{B.3}$$

and $\boldsymbol{f}_L$ is the volumetric Lorentz force. The equation of motion for the combined ion-neutral fluid is found by addition of Equations B.1 and B.2

$$\rho \boldsymbol{a} = \rho \boldsymbol{g} + \boldsymbol{f}_L \tag{B.4}$$

where $\rho \equiv \rho_n + \rho_i$ is the mass density without the electrons and $\boldsymbol{a} \equiv (\rho_n \boldsymbol{a}_n + \rho_i \boldsymbol{a}_i)/\rho$ is the total acceleration.

The gravitational acceleration term can then be eliminated from Equations B.1 and B.2 to give

$$\boldsymbol{a}_n - \boldsymbol{a}_i = \left(\frac{1}{\rho_n} + \frac{1}{\rho_i}\right) \boldsymbol{f}_d - \frac{1}{\rho_i} \boldsymbol{f}_L. \tag{B.5}$$

Assuming then that the acceleration of the neutrals and ions are the same we get

$$\boldsymbol{f}_d = \left(\frac{\rho_n}{\rho_n + \rho_i}\right) \boldsymbol{f}_L. \tag{B.6}$$

This equation tells us that for a lightly ionized outflow the drag force is almost equal to the Lorentz force. We can now obtain an expression for the slip velocity, $\boldsymbol{w}$, by subbing this equation into Equation B.3

$$\boldsymbol{w} = \boldsymbol{v}_i - \boldsymbol{v}_n = \frac{\boldsymbol{f}_L}{\gamma \rho_i (\rho_n + \rho_n)}. \tag{B.7}$$

The slip velocity becomes large when the ion density becomes small, but does not become large when the neutral density becomes small because the large density of ions drag the few neutrals that are present along with the rest of the mostly ionized plasma. The heating rate per unit volume due to ambipolar diffusion heating is

$$\Gamma = \boldsymbol{f}_d . \boldsymbol{w} \tag{B.8}$$

and substitution of Equations B.6 and B.7 gives

$$\Gamma = \frac{\rho_n |\boldsymbol{f}_L|^2}{\gamma \rho_i (\rho_n + \rho_i)^2}, \tag{B.9}$$

and so for a completely ionized plasma, $\Gamma = 0$.

In order to calculate the ambipolar diffusion heating, we need to find a value for the ion-neutral momentum transfer coefficient, γ (in units $\mathrm{cm^3\,s^{-1}\,g^{-1}}$) which depends on the collisional coefficient rates, cross sections, slip speed, and gas

composition. Shang *et al.* (2002) give the following expression

$$\gamma = \frac{2.13 \times 10^{14}}{1 - 0.714 x_e} \left(\left[3.23 + 41.0 T_4^{0.5} \times \left(1 + 1.338 \times 10^{-3} \frac{w_5^2}{T_4} \right)^{0.5} \right] x_{HI} + 0.243 \right) \tag{B.10}$$

where T_4 is the temperature in units of $10^4\,\mathrm{K}$, w_5 is the slip speed in units of $\mathrm{km\,s^{-1}}$. We have assumed no molecular hydrogen to be present and the fractional abundance of He, $x_{He} = 0.1$. Subbing Equation B.7 into Equation B.10 gives a quartic equation for γ, i.e.,

$$\begin{aligned} \gamma^4 - (2AE + 2ABx_{HI})\gamma^3 + (A^2E^2 + 2A^2BEx_{HI} + \\ A^2B^2x_{HI}^2 - A^2C^2x_{HI}^2)\gamma^2 - GA^2C^2x_{HI}^2 = 0 \end{aligned}$$

where
$A = \frac{2.13\times10^{14}}{1-0.714x_e}$, $B = 3.23$, $C = 41.0T_4^{0.5}$, $D = \frac{1.338\times10^{-3}}{T_4}$, $E = 0.243$, $F = \frac{\boldsymbol{f}_L}{\rho_i(\rho_n+\rho_i)}$, and $G = \frac{DF^2}{1\times10^{10}}$. Finally the radial and azimuthal Lorentz forces and thus the corresponding volumetric ambipolar heating rates can be calculated by using the following expressions for the flow and gravitational accelerations:

$$\boldsymbol{a} = v\frac{dv}{dr}\boldsymbol{r} + \frac{v}{r}\frac{dv}{d\theta}\boldsymbol{\theta} \tag{B.11}$$

and

$$\boldsymbol{g} = -\frac{GM_\star}{r^2}\boldsymbol{r} + \frac{1}{r}\frac{d}{d\theta}\left(\frac{GM_\star}{r}\right)\boldsymbol{\theta}. \tag{B.12}$$

References

Adams, W.S. & MacCormack, E. (1935). Systematic Displacements of Lines in the Spectra of Certain Bright Stars. *Astrophysical Journal*, **81**, 119. (Cited on page 4.)

Altenhoff, W.J., Mezger, P.G., Wendker, H.J. & Westerhout, G. (1960). Veröff. Sternwärte, Bonn. **59**, 48. (Cited on page 10.)

Ayres, T.R., Linsky, J.L., Vaiana, G.S., Golub, L. & Rosner, R. (1981). The cool half of the H-R diagram in soft X-rays. *Astrophysical Journal*, **250**, 293–299. (Cited on pages 2 and 4.)

Ayres, T.R., Brown, A., Harper, G.M., Bennett, P.D., Linsky, J.L., Carpenter, K.G. & Robinson, R.D. (1997). Digging Deeper in the Coronal Graveyard. *Astrophysical Journal*, **491**, 876. (Cited on page 4.)

Carpenter, K.G., Robinson, R.D., Harper, G.M., Bennett, P.D., Brown, A. & Mullan, D.J. (1999). GHRS Observations of Cool, Low-Gravity Stars. V. The Outer Atmosphere and Wind of the Nearby K Supergiant lambda Velorum. *Astrophysical Journal*, **521**, 382–406. (Cited on page 4.)

Chiosi, C. & Maeder, A. (1986). The evolution of massive stars with mass loss. *Annual Review of Astronomy & Astrophysics*, **24**, 329–375. (Cited on page 2.)

Crowley, C., Espey, B.R., Harper, G.M. & Roche, J. (2009). Winds and Chromospheres of Cool (Super-) Giants. In E. Stempels, ed., *15th Cambridge Workshop on Cool Stars, Stellar Systems, and the Sun*, vol. 1094 of *American Institute of Physics Conference Series*, 267–274. (Cited on pages 2 and 3.)

Deutsch, A.J. (1956). The Circumstellar Envelope of Alpha Herculis. *Astrophysical Journal*, **123**, 210. (Cited on page 4.)

Drake, S. & Linsky, J. (1986). Radio continuum emission from winds, chromospheres, and coronae of cool giants and supergiants. *Astronomical Journal*, **91**, 602–620. (Cited on page 14.)

Dupree, A.K., Lobel, A., Young, P.R., Ake, T.B., Linsky, J.L. & Redfield, S. (2005). A Far-Ultraviolet Spectroscopic Survey of Luminous Cool Stars. *Astrophysical Journal*, **622**, 629–652. (Cited on page 4.)

Eaton, J.A. (2008). A Model for the Chromosphere/Wind of 31 Cygni and Its Implications for Single Stars. *Astronomical Journal*, **136**, 1964–1979. (Cited on page 3.)

REFERENCES

Falceta-Gonçalves, D., Vidotto, A.A. & Jatenco-Pereira, V. (2006). On the magnetic structure and wind parameter profiles of Alfvén wave driven winds in late-type supergiant stars. *Monthly Notices of the Royal Astronomical Society*, **368**, 1145–1150. (Cited on page 3.)

Gradshteyn, I.S. & Ryzhik, I.M. (1994). *Table of integrals, series and products*. (Cited on page 14.)

Güdel, M. (2002). Stellar Radio Astronomy: Probing Stellar Atmospheres from Protostars to Giants. *Annual Review of Astronomy & Astrophysics*, **40**, 217–261. (Cited on page 5.)

Haisch, B.M., Linsky, J.L. & Basri, G.S. (1980). Outer atmospheres of cool stars. IV - A discussion of cool stellar wind models. *Astrophysical Journal*, **235**, 519–533. (Cited on page 2.)

Harper, G.M. (1988). *The outer atmospheres of hybrid giants*. Ph.D. thesis, Oxford Univ. (England). (Cited on page 2.)

Harper, G.M. (2010). Betelgeuse: A Case Study of an Inhomogeneous Extended Atmosphere. In C. Leitherer, P.D. Bennett, P.W. Morris & J.T. Van Loon, eds., *Hot and Cool: Bridging Gaps in Massive Star Evolution*, vol. 425 of *Astronomical Society of the Pacific Conference Series*, 152. (Cited on page 3.)

Harper, G.M., Brown, A. & Lim, J. (2001). A Spatially Resolved, Semiempirical Model for the Extended Atmosphere of α Orionis (M2 Iab). *Astrophysical Journal*, **551**, 1073–1098. (Cited on page 2.)

Hartmann, L. & MacGregor, K.B. (1980). Momentum and energy deposition in late-type stellar atmospheres and winds. *Astrophysical Journal*, **242**, 260–282. (Cited on page 2.)

Holzer, T.E. & MacGregor, K.B. (1985). Mass loss mechanisms for cool, low-gravity stars. In M. Morris & B. Zuckerman, eds., *Mass Loss from Red Giants*, vol. 117 of *Astrophysics and Space Science Library*, 229–255. (Cited on page 2.)

Hummer, D.G. (1988). A fast and accurate method for evaluating the nonrelativistic free-free Gaunt factor for hydrogenic ions. *Astrophysical Journal*, **327**, 477–484. (Cited on page 10.)

Jones, M.H. (2008). The incidence of mid-infrared excesses in G and K giants. *Monthly Notices of the Royal Astronomical Society*, **387**, 845–855. (Cited on page 2.)

Judge, P.G. & Carpenter, K.G. (1998). On Chromospheric Heating Mechanisms of "Basal Flux" Stars. *Astrophysical Journal*, **494**, 828. (Cited on page 2.)

Linsky, J.L. & Haisch, B.M. (1979). Outer atmospheres of cool stars. I - The sharp division into solar-type and non-solar-type stars. *Astrophysical Journal Letters*, **229**, L27–L32. (Cited on pages 2 and 4.)

Newell, R.T. & Hjellming, R.M. (1982). Radio emission from the extended chromosphere of Alpha Orionis. *Astrophysical Journal Letters*, **263**, L85–L87. (Cited on pages 14 and 15.)

Reimers, D. (1982). Detection of further red giants with 'hybrid' atmospheres and a possible correlation with double circumstellar MG II and CA II lines. *Astronomy & Astrophysics*, **107**, 292–299. (Cited on page 4.)

Rohlfs, K. & Wilson, T.L. (1996). *Tools of Radio Astronomy*. (Cited on page 7.)

Schröder, K.P. & Sedlmayr, E. (2001). The galactic mass injection from cool stellar winds of the 1 to 2.5 M_{sun} stars in the solar neighbourhood. *Astronomy & Astrophysics*, **366**, 913–922. (Cited on page 2.)

Shang, H., Glassgold, A.E., Shu, F.H. & Lizano, S. (2002). Heating and Ionization of X-Winds. *Astrophysical Journal*, **564**, 853–876. (Cited on page 20.)

Spitzer, L., Jr. (1939). Spectra of M Supergiant Stars. *Astrophysical Journal*, **90**, 494. (Cited on page 4.)

Sutmann, G. & Cuntz, M. (1995). Generation of mass loss in K giants: The failure of global oscillation modes and possible implications. *Astrophysical Journal Letters*, **442**, L61–L64. (Cited on page 2.)

Suzuki, T.K. (2007). Structured Red Giant Winds with Magnetized Hot Bubbles and the Corona/Cool Wind Dividing Line. *Astrophysical Journal*, **659**, 1592–1610. (Cited on page 3.)

van Loon, J.T. (2010). The Effects of Red Supergiant Mass Loss on Supernova Ejecta and the Circumburst Medium. In C. Leitherer, P.D. Bennett, P.W. Morris & J.T. Van Loon, eds., *Hot and Cool: Bridging Gaps in Massive Star Evolution*, vol. 425 of *Astronomical Society of the Pacific Conference Series*, 279. (Cited on page 2.)

Zuckerman, B., Kim, S.S. & Liu, T. (1995). Luminosity Class III Stars with Excess Far-Infrared Emission. *Astrophysical Journal Letters*, **446**, L79. (Cited on page 2.)